Copernicus Climate Change

# Integration of Climate Data in the SAVi Buildings Model

## C3S_428h_IISD-EU: Sustainable Asset Valuation (SAVi): Demonstrating the Business Case for Climate-Resilient and Sustainable Infrastructure

Issued by: IISD-EU / Oshani Perera

Date: September 2020

Ref:

C3S_428h_IISD-EU_D428h.1.1 _202006_Integration of climate data in the SAVi model_v2

Official reference number service contract:

2019/C3S_428h_IISD-EU/SC1

IMPLEMENTED BY ECMWF

# Contributors


**International Institute for Sustainable Development**
Bechauf, Ronja
Casier, Liesbeth
Lago, Sergio
Perera, Oshani
Perrette, Mahé
Uzsoki, David
Wuennenberg, Laurin

**KnowlEdge Srl**
Bassi, Andrea M.
Pallaske, Georg

## Table of Contents

# 1 About This Report

This report outlines the integration of authoritative Copernicus Climate Data from the Climate Data Store (CDS) into a Sustainable Asset Valuation (SAVi) of building infrastructure. It describes how several climate indicators obtained from the CDS were integrated into the SAVi Buildings model and how the analysis performed by SAVi has improved as a result. In light of this integration, IISD is able to generate sophisticated SAVi-derived analyses on the costs of climate-related risks and climate-related externalities.

The integration of Copernicus Climate Data into other SAVi models for energy, irrigation, wastewater treatment infrastructure, roads, and nature-based infrastructure can be found here.

This document presents:

- A summary of the literature review on the climate impact on buildings, including the equations that link climate variables to the performance of buildings.
- How the above information was used to select relevant indicators from the Copernicus database.
- How outputs of the CDS datasets are integrated into the SAVi System Dynamics (SD) Buildings model.
- How simulation results can be affected by the use of this new and improved set of indicators.

This report is organized as follows.

**Literature Review**

The literature review contains the following subsections for each of the climate variables discussed for buildings:

- Subsection 1: An overview of climate impacts on the asset (e.g., temperature change affects the energy consumption of a building).
- Subsection 2: A presentation of papers/reports that provide case studies that summarize the range of impacts estimated or observed (e.g., across countries).
- Subsection 3: A description of the methodology found in the literature for the calculation of climate impacts on buildings.
- Subsection 4: A selection of CDS datasets required by the equations.

**Integration of the Literature Review with the CDS Dataset**

This section summarizes information on which datasets are being used from the Copernicus database and what additional processing was applied before integration into the SAVi Buildings model for each asset. We first review the equations to determine their usefulness for SAVi models. We assess what data requirements for each of the equations are available in the Copernicus database and create indicators for climate variables that are relevant for the equations selected. Finally, in certain cases, we create indicators in the CDS Toolbox for first-order impacts on infrastructure. Second- and third-order impacts will be estimated with SAVi, making use of additional equations included in the SD model.

**Integration of Climate Indicators Into the SAVi Buildings Model**

This section explains how the CDS indicators are integrated in the SAVi SD Buildings model. It includes an identification of the specific performance indicators of building projects impacted by climate indicators (e.g., efficiency and cost).

**Behavioural Impacts Resulting From the Integration of Climate Variables**

This section discusses how climate variables affect asset performance in the SD model, providing early insights as to how the results of the SAVi analysis may change when equipping the model with more and better refined climate indicators (e.g., with the cost of infrastructure being higher due to increased maintenance, the economic viability of the infrastructure asset, presented as the Internal Rate of Return [IRR], will be lower than expected).

**Simulation Results**

The final section of this paper presents the equations used and quantitative results emerging from the inclusion of climate indicators in the SAVi Buildings model under various climate scenarios. This is the end product of the enhanced SAVi Buildings model, which is used to inform policy and investment decisions for infrastructure.

Table 1 provides an overview of climate drivers, impacts, and relevant SAVi output indicators of the SAVi Buildings model.

The CDS datasets are accessed via the CDS application programming interface (API), and additional processing and packaging for use in SAVi is done offline. Technical information about the offline code is found in Annex I.

We also selected a subset of the most-used indicators and created an app in the CDS Toolbox with interactive visualization for demonstration purposes.

Table 1. Overview of variables and impacts implemented in the SAVi Buildings model

| SAVi module | Implemented impact | Main climate drivers | Affected output indicators |
|---|---|---|---|
| **Buildings** | Stormwater harvesting yield | • Precipitation | • Water use in buildings<br>• Water cost |
| | Effect of temperature on the load factor of rooftop solar photovoltaic (PV) | • Temperature | • Solar PV generation<br>• Electricity cost<br>• Emissions from electricity use<br>• Social cost of carbon |
| | Heating degree days | • Temperature | • Heating energy expenditure<br>• Heating energy use<br>• Emissions from electricity use<br>• Social cost of carbon |
| | Cooling degree days | • Temperature | • Cooling energy expenditure<br>• Cooling energy use<br>• Emissions from electricity use<br>• Social cost of carbon |

# 2 Buildings

## 2.1 Literature review

### 2.1.1 Energy demand and efficiency

#### 2.1.1.1 Heating and cooling degree days

Higher temperature increases the demand for cooling days. Lower temperature increases the need for heating days. Depending on the level of thermal insulation of the building, more energy will be required for indoor thermal regulation.

- **Climate impact**

Heating degree day (HDD) index is a weather-based technical index designed to describe the need for the heating energy requirements of buildings. Cooling degree day (CDD) index is a weather-based technical index designed to describe the need for the cooling (air conditioning) requirements of buildings. Both have an impact on energy demand and building isolation efficiency.

- **Summary of results**

In a case study in L.A, it has been estimated that for every 1˚C increase in temperature, electricity demand would increase in the range of 2–4% for the whole network. Another study estimated the per capita increase for Guangzhou, China. It found that, on average, an increase of 1˚C would lead to an increase of electricity demand between 0.015 and 0.02% during the year with fluctuations between summer and winter.

- **Results**

Akbari (2005) found that on a clear summer afternoon, the air temperature in a typical city is as much as 2.5K higher than in the surrounding rural areas. It has been shown that peak urban electric demand rises by 2– 4% for each 1K rise in daily maximum temperature above a threshold of 15–20°C. Thus, the additional air-conditioning use caused by this urban air temperature increase is responsible for 5–10% of urban peak electric demand.

In rural China, Zhang et al. (2019) found out that by using the statistics of counties from 2006 to 2015 in a fixed-effect panel model, the results indicate that a one-degree temperature increase in summer days may lead to 0.015% more electricity consumption per capita, and this correlation may be weaker as income increases. Moreover, a one-degree temperature decrease in winter days may lead to 0.002% more electricity consumption. The northern region may consume 0.021% more electricity than the southern region when facing the same temperature drop.
Threshold for cooling and heating degree days is set at 5 °C for heating and 26 °C for cooling.

Also in Guangzhou, China, Zheng et al. (2020) estimated that with a higher temperature of 1 °C, total electricity consumption would increase by 2.7%, and the residential one would increase by 0.9%. In addition, the projected impacts of climate change on electricity consumption would depend on the emissions of greenhouse gases. In other words, electricity consumption would vary significantly under four RCPs, with the impacts being increased gradually from RCP2.6 to RCP8.5

- **Methodology**

Method 1 (De Rosa, Bianco, Scarpa, & Tagliafico, 2014)

The degree-days method is based on the assumption that energy consumption is proportional to the difference between external and internal temperature:

1. Therefore, assuming a global building transmission coefficient H in W/K, the monthly energy consumption Em can be calculated as follows:

$$E_m = \frac{H \cdot DD_m \cdot t_h}{\eta_{hs/cs}}$$

Where $t_h$ is the heating time in a day (which can be assumed equal to 24 h if a continuous heating/cooling is provided), $\eta_{hs/cs}$ is the efficiency of the equipment, and $DD_m$ is the total heating or cooling degree days of a month m.

$$\text{Heating}: \quad DD_m = \text{HDD}_m = \sum_{d=1}^{D_m} (T_{b,hs} - \overline{T}_{e,d})^+$$

$$\text{Cooling}: \quad DD_m = \text{CDD}_m = \sum_{d=1}^{D_m} (\overline{T}_{e,d} - T_{b,cs})^+$$

$T_{e,d}$ represents the mean of the daily maximum and minimum external air temperature of a day d $T_{b,hs}$ and $T_{b,cs}$ are the base temperatures for heating and cooling respectively, which represent the temperature set point of the inner heated/cooled zones.

The sign + indicates that only positive values are added. Different approaches can be adopted to calculate the degree days, depending on the type of data available for the external temperature.

Cooling degree days modified for low values:

In order to restore the validity of CDDs for low values, a simple correction is introduced. Starting from the standard CDD, provided:

$$\text{CDD}^* = \text{CDD} + \chi \cdot I_{t0,y}$$

Where $I_{t0, y}$ is the total horizontal solar irradiation of each locality, computed by summing the daily values only when a cooling demand is necessary, while $\chi$ is the correction factor, which is adjusted in order to minimize the deviation of the linear regression.

A short review of the different techniques is reported in an article made by Mourshed (2012) while a simple application can be found in another article by Büyükalaca et al. (2001).

Method 2 (Eurostat, the Statistical Office of the European Union, 2019)

HDD: If Tm ≤ 15°C Then [HDD = ∑i(18°C - Tim)] Else [HDD = 0] where Tim is the mean air temperature of day i.

CDD: If Tm ≥ 24°C Then [CDD = ∑iTim - 21°C)] Else [CDD = 0] where Tim is the mean air temperature of day i.

**Considerations for integration in the CDS toolbox**

Air temperature (K): ERA5-Land hourly data from 1981 to present & CMIP5 daily data on pressure levels can be used to estimate the previous equations.

#### 2.1.1.2 Albedo/Temperature of a surface

- **Climate impact**

High temperatures are responsible for the increase of energy demand for air conditioning in buildings and photochemistry effects that increase atmospheric pollution, as well as increasing environmental impacts due to the demand of energy generation. Materials with high albedo and emittance attain lower temperatures when exposed to solar radiation, reducing the transference of heat to the environmental air (Prado & Ferreira, 2005).

- **Methodology**

Equation for determining the temperature for a surface under the sun (Prado & Ferreira, 2005):

$$(1 - a)I = \sigma \times \varepsilon \times (T^4_{s} - T^4_{sky}) + h_c \times (T_s - T_a)$$

where a is the albedo or solar reflectance; I the incident solar radiation on the surface (W/m2); ε the emittance of the surface; σ the constant of Stefan–Boltzmann ($5.67 \times 10^{-8}$ W/m$^2$ K$^4$); $T_s$ the balance temperature of the surface (K or ˚C); $T_{sky}$ the radiating temperature of the sky (K or ˚C); $h_c$ the convection coefficient (W/m$^2$ K or W/m$^2$ ˚C); $T_a$ the temperature of air (K or ˚C)

**Considerations for integration in the CDS toolbox**

Albedo: Dimensionless - ERA5-Land monthly averaged data from 1981 to present
Solar radiation: J /m$^2$ - ERA5-Land monthly averaged data from 1981 to present
Temperature of air: K - ERA5-Land monthly averaged data from 1981 to present

#### 2.1.1.3 Soil temperature / Moisture

- **Climate impact**

Soil temperature and moisture have an impact on how much energy is evacuated through soils and hence affect indoor temperature, and related cooling and heating needs.

- **Methodology**

In a paper by Janssen et al. (2004), the influence of soil moisture transfer on building heat loss via the ground is investigated by comparing fully coupled simulations with linear thermal simulations. The observed influences of coupling are:
- The larger amplitude of surface temperature
- The variation of thermal conductivity with moisture content
- The advection of sensible heat by liquid transfer.

Surface heat balance ($q_{h,se}$) and Moisture balance ($q_{m,se}$) are given:

$$q_{\mathrm{h,se}} = H + R_{\mathrm{t}} + \mathrm{LE} + \mathrm{HP},$$

$$q_{\mathrm{m,se}} = E + P.$$

Where heat exchange (H), solar and long-wave radiation ($R_t$), and the transfer of sensible and latent heat by evaporation (LE) and precipitation (HP). Precipitation (P) and evaporation (E).

**Considerations for integration in the CDS toolbox**

Radiation, evaporation, precipitation: ERA5 monthly averaged data on single levels from 1979 to present

### 2.1.2 Rainwater harvest

Rainwater harvest is a common feature of buildings, either new ones or those located in areas prone to drought.

#### 2.1.2.1 Precipitation

- **Climate impact**

Precipitation and the roof area of buildings are the main determinants of rainwater harvesting.

- **Methodology**

Method 1 (Pande & Telang, 2014)

Estimation of mean rainwater supply that could be used for buildings or any other infrastructure.

Mean rainwater supply in $m^3$ =
Mean annual rainfall in m/year × Surface area of catchment in $m^2$ × Run-off coefficient

**Considerations for integration in the CDS toolbox**

Rainfall: m - ERA5 monthly averaged data on single levels from 1979 to present
Run-off: m - ERA5-Land monthly averaged data from 1981 to present

Method 2 (Diaz, Osmond, & King, 2015)

This method supplements existing climate analysis tools by defining a scale and benchmarks that easily link potential water requirements of buildings with water availability from precipitation.
It is necessary to associate the units of precipitation with those of water demand. The relation of precipitation and water demand scales is influenced by the runoff efficiency of the roof or other element from which the water is collected.

Precipitation Benchmark: minimum level of precipitation required for a building to fully meet its demand of rainwater, and any amount above this level is exceeding precipitation which could be stored by the building for future needs:

PB = (Dt x 30 days) / ([CRa/HFa] x C) *(1)*

PB = Precipitation benchmark (mm or L/$m^2$)
Dt = Total water demand (L/$m^2$ day)
CRa = Collectable roof Area ($m^2$)
HFa = Habitable floor area ($m^2$)
C = Runoff Coefficient (dimensionless)
The denominator in equation *(1)* is termed the Building Factor (BF), because all its variables depend on the configuration of the building. The minimum precipitation required to satisfy the water demand of the building will vary according to its BF (the requirement increases when BF is 1).

If water is required for different purposes (e.g. laundry, toilets, EC, etc.) DT must be calculated previously with the formula:

Dt = De + (Da/HFa) *(2)*

De = Water demand for EC (L/$m^2$ day)
Da = Supplementary water demand (L/day)

This water demand may vary according to the climate and the specific needs of each building. Even very similar buildings may have differences in the amounts of water required (e.g. due to orientation, surrounding influences, etc.). Thus, the particular demand of a building must be individually calculated

**Considerations for integration in the CDS toolbox**

ERA5 monthly averaged data on single levels from 1979 to present
ERA5-Land monthly averaged data from 1981 to present

### 2.1.3 Climate hazards

A building (a type of physical infrastructure) is impacted by extreme events related to wind, water and temperature. Depending on the type of building and technology, construction materials and strength of construction, impacts will vary.

#### 2.1.3.1 Flood discharge

- **Climate impact**

Floods have an impact on buildings due mainly to water penetration and hence flooding.

- **Methodology**

Assessing the impact of flood damage (JICA, March 2003):

$$Q_p = \frac{ciA}{3.6}$$

Where: $Q_p$ = maximum flood discharge ($m^3/s$)
$c$ = dimensionless runoff coefficient
$i$ = rainfall intensity within time $t_c$
$A$ = catchment area ($km^2$)

The computed peak rate of runoff at the outlet point is a function of the average rainfall rate during the time of concentration, i.e., the peak discharge does not result from a more intense storm of shorter duration, during which only a portion of the watershed is contributing to the runoff at the outlet.
The time of concentration employed is the time for the runoff to become established and flow from the most remote part of the drainage area to the outlet point. Rainfall intensity is constant throughout the rainfall duration

**Considerations for integration in the CDS toolbox**

ERA5 monthly averaged data on single levels from 1979 to present
ERA5-Land monthly averaged data from 1981 to present

#### 2.1.3.2 Wind pressure

- **Climate impact**

Overhangs from a building are affected by wind pressure acting from underneath. These combined with pressures (or suctions) on the top surface often create a severe design condition. (Krishna, Kumar, & Bhandari, 2002)

- **Methodology**

The wind pressure at any height above mean ground level shall be obtained by the following relationship between wind pressure and wind speed (Krishna, Kumar, & Bhandari, 2002):

$$P_z = 0.6 \times V_z^2$$

Where $P_z$ = wind pressure in N/m2 at height z, and $V_z$ = design wind speed in m/s at height z. The relationship between design wind speed $V_z$ and the pressure produced by it assumes the mass density of air as 1.20 $kg/m^3$, which changes somewhat with the atmospheric temperature and pressure.

**Considerations for integration in the CDS toolbox**

Wind speed: m/s - ERA5 monthly averaged data on single levels from 1979 to present

#### 2.1.3.3 Lightning

- **Climate impact**

Lightning can cause damage to a building's infrastructure. Material damages of course, electrical damages to cables and electricity infrastructure that might cause power shutdown.

- **Summary of results**

Literature is very scarce but we found that for every 1˚C rise in global temperatures, there will be an increase of 12% in the frequency of lightning strikes.

- **Results**

Costs and damages of lightning in the US as published by Vought (2019), costs about $1,200 per year or $100 per month for facility lightning protection. Yet it can prevent infrastructure failure costing as much as $100,000 per hour. Lightning are likely to increase as shown with the equation he provides:

$$F = \text{constant} \times P \times CAPE$$

With F = flash rate per area; P=precipitation rate; CAPE=convective potential available energy (potential electrical energy of that area -> increases with higher temperatures as reflected by the ability of air of rising more rapidly into the upper atmosphere).

In the web page of Sollatek (2016), a firm specialized in lightning equipment, we can read that for every 1˚C rise in global temperatures, there will be an increase of 12% in the frequency of lightning strikes. With that said we can expect to see a 50% rise in the next 100 years. For every two lightning strikes in 2000, there will be three lightning strikes in 2100.

## 2.2 Integration of literature review with the CDS datasets

See section 1.2 for explanations how we selected the indicators to implement in the CDS Toolbox.

<u>Datasets</u>:

- ERA5 monthly data on single level
- CMIP5 monthly data on single level
- ERA5 hourly data on single level

<u>Indicators created</u>:

- **Air temperature**
  - Units: degrees Celsius
  - Frequency: monthly
  - ERA5 variable: “2 m temperature”
  - CMIP5 variable: “2 m temperature“
  - Note: original units in Kelvin
- **Precipitation**:
  - Units: mm per month
  - Frequency: monthly
  - ERA5 variable: “Mean total precipitation rate”
  - CMIP5 variable: “Mean precipitation flux“
  - Note different: units scaling was necessary
  - CMIP5 variable: “2m_temperature “
- **Min Daily temperature**
  - Units: degrees Celsius
  - Frequency: monthly
  - ERA5 variable: “2m temperature”
    - Daily min and monthly mean from hourly temperature
  - CMIP5 variable: “minimum_2m_temperature_in_the_last_24_hours “
- **Max Daily temperature**
  - Units: degrees Celsius
  - Frequency: daily
  - ERA5 variable: “2m temperature”
    - Daily max and monthly mean from hourly temperature

- CMIP5 variable: “maximum_2m_temperature_in_the_last_24_hours “
- **Wind**
  - Units: m/s
  - Frequency: monthly
  - ERA5 variable: “10 m wind speed”
  - CMIP5 variable: “10 m wind speed“

<u>Additional information</u>

Daily temperature indices may be useful to determine heating degree day and cooling degree day indices.

## 2.3 Integration of climate indicators into the SAVi buildings model

The climate indicators developed in, and extracted from the toolbox, include impacts on heating and cooling, lighting, rooftop solar generation and rainwater harvesting. We have also estimated climate hazards related to flood and wind pressure. The CLD for buildings is presented in Figure 44.

Figure 1 Causal Loop Diagram for the buildings sector - CDS variables included

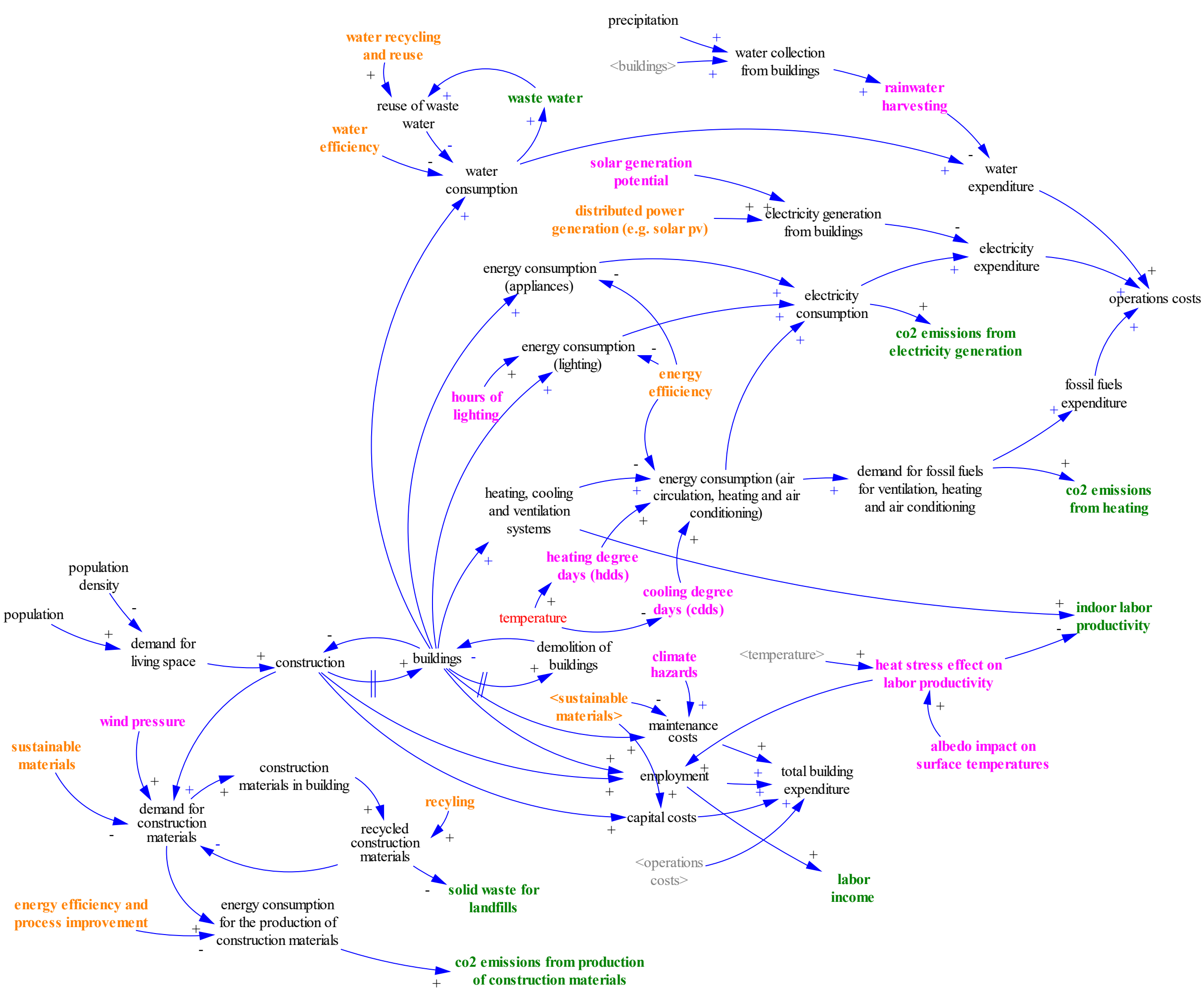

The time duration of heating and cooling in the SAVi model is defined as a function of Heating Degree Days (HDD) and Cooling Degree Days (CDD), which are obtained from the CDS toolbox. In the model, HDDs determine the days of the year during which buildings are heated. CDDs, on the other hand, determine the number of days during which air-conditioning is required. HDD and CDD therefore affect energy consumption, energy costs and emissions (depending on the technology used), having an impact on both operation cost and societal costs.

The hours of lighting, used to determine energy consumption for lighting, are obtained from the CDS toolbox. The further away from the equator the project is located, the more seasonal and total difference in lighting hours have to be considered. The energy requirements for lighting affect energy costs, and hence the cost of operation of the building and, indirectly air emissions (depending on the technology and energy source used to produce electricity).

The rooftop solar power generation potential represents the amount of electricity that can be generated using rooftop solar PV. Solar generation depends on solar radiation (resulting from location, sunshine hours and cloud cover). The CDS toolbox provides the projected solar power generation potential by location, and the SAVi model uses it to determine the specific electricity generation for the project considered.  This takes into account the size of the PV installation, and reduced the purchase of electricity, its cost and air emissions.

The rainwater harvesting potential is the amount of water that could be harvested by a building, given a specific technology and related efficiency. Rainwater harvesting reduces building water demand and contributes to lowering potable water use. The rainwater harvesting potential is estimated by the CDS toolbox and used as an input to SAVi.

The impact of floods and wind pressure are considered to determine the integrity of the building, and any potential damage top physical infrastructure and related costs.

## 2.4 Behavioral impacts resulting from the integration of climate variables

Obtaining HDDs and CDDs from the toolbox allows for projecting future heating and cooling requirements and seasonal peaks more accurately. This improves both the estimation of capacity requirements for heating and cooling and related costs. It further allows a more accurate assessment of the effectiveness and economic viability of different solutions for heating and cooling as well as thermal insulation.

Information concerning the hours of lighting allows to model lighting requirements and related energy consumption and cost more accurately. Changes in lighting requirements also lead to changes in the use of light bulbs, and hence improving the estimation of replacement rates and related cost.

Location-specific forecasts of solar power generation potential improves the projection of rooftop PV power generation and economic viability in the SAVi model. Changes in solar generation potential affect revenues from feed in tariffs as well as the amount of grid-based electricity is consumed. Grid-based electricity consumption affects user costs and total building related CO2e emissions.

The rainwater harvesting potential generated by the CDS toolbox improves the estimation of the monthly water requirement and purchase from water utilities. It also allows SAVi to make use of various climate change forecasts with daily/weekly/monthly time steps, a new feature for the estimation of this indicator. This greatly enhances the potential for SAVi to be used in areas prone to drought, and to assess the climate resilience of buildings more fully.

Floods and extreme wind pressure support the estimation of extraordinary maintenance costs in the model. This information will highlight how constructing new buildings in disaster-prone areas may not be financially viable.

## 2.5 Simulation results

The literature review above has shown that climate impacts buildings in various ways. Three CDS based climate variables were integrated into the SAVi Buildings model, (1) rainwater harvesting potential per m2, (2) heating and cooling degree days, and (3) the effect of temperature on rooftop solar PV generation.

### 2.5.1 Rainwater harvesting potential

Rainwater harvesting potential refers to the amount of rainwater that can be collected given that infrastructure for rainwater harvesting is in place. In most cases, the collected rainwater is used to substitute potable water for a variety of uses such as gardening, toilet flushing and others.

The amount of rainwater that can be collected depends on the available area (in m2) for rainwater harvesting, the runoff coefficient of the roof surface and seasonal precipitation. The following equation is used for calculating potential rainwater harvesting yield based on CDS data, based on Biswas (2014).

*Rainwater harvesting potential = Monthly precipitation * Runoff coefficient * Conversion mm to liter per m2*

Figure 45 provides an overview of runoff coefficients for various roofing materials. As provided by Biswas (2014). For the results presented below, a runoff coefficient of 0.8 is applied.

| Type | Runoff coefficient |
|---|---|
| Galvanized iron sheet | >0.9 |
| Corrugated metal sheet | 0.7–0.9 |
| Tiles | 0.8-0.9 |
| Concrete | 0.6–0.8 |
| Brick pavement | 0.5-0.6 |
| Rocky natural catchment | 0.2–0.5 |
| Soil with slope | 0.0–0.3 |
| Green area | 0.05–0.1 |

Figure 2: Rainwater runoff coefficients for various roofing materials (Biswas, 2014)

The results of rainwater harvesting potential in the no climate and climate impact scenario is presented in Figure 46. The results show that the previous formulation used in SAVi is significantly underestimating the potential for rainwater harvesting.

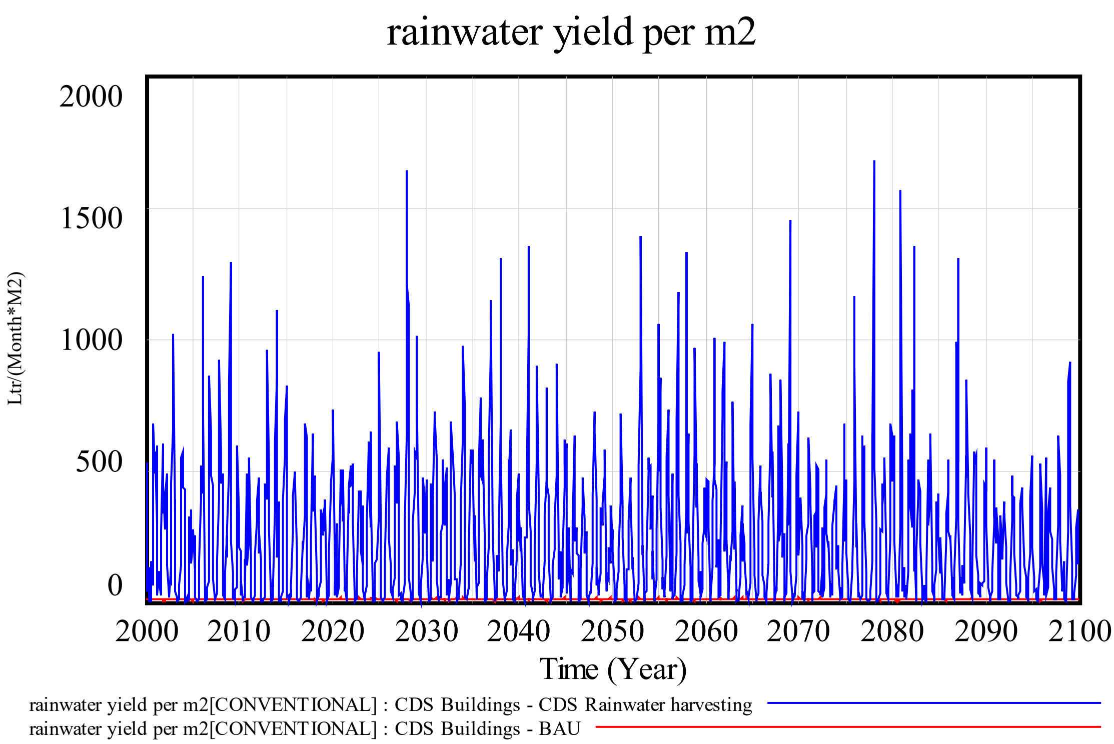


Figure 3: Rainwater harvesting yield per m2 of roof surface

The use of climate data to forecast rainwater harvesting yields compared to using constant seasonal precipitation values in the no climate scenario yields significant differences. Between

2020 and 2100, the average annual rainwater harvesting yield is 134.7 liters per m2 in the no climate scenario and 3,068.6 liters per m2 in the CDS climate scenario. The difference in annual averages indicates that the yield forecasted by climate data-based formulations is almost 23 times higher compared to the no climate scenario.

Furthermore, the maximum monthly value for rainwater harvesting yields indicated in the no climate and CDS climate impact scenario is 15.2 liter per m2 and 1,674.9 liters per m2 respectively. Table 17 compares the average monthly rainwater harvesting yields in the CDS climate and the no climate scenario respectively.

| **Rainwater yield in liter per m2** | **2020-2030** | **2030-2040** | **2040-2050** | **2050-2060** | **2060-2070** | **2070-2080** | **2080-2090** | **2090-2100** |
|---|---|---|---|---|---|---|---|---|
| CDS climate scenario | 275.41 | 286.10 | 247.46 | 272.25 | 270.34 | 235.02 | 258.96 | 196.39 |
| *CDS relative to 2020-2030* | *0.0%* | *3.9%* | *-10.1%* | *-1.1%* | *-1.8%* | *-14.7%* | *-6.0%* | *-28.7%* |
| No climate scenario | 11.48 | 11.49 | 11.01 | 10.83 | 11.17 | 11.54 | 10.81 | 11.37 |
| *No climate relative to 2020-2030* | *0.0%* | *0.0%* | *-4.1%* | *-5.7%* | *-2.8%* | *0.5%* | *-5.8%* | *-1.0%* |

Table 2: Average rainwater harvesting yield per decade

Between 2020 and 2100, the cumulative amount of rainwater that can potentially be harvested is 10,774 liters per m2 in the no climate scenario and 245,491 liters per m2 in the CDS climate impact scenario respectively. Assuming that one liter of water costs 0.5 cents, the projected net savings in water expenditure over 80 years total EUR 53.87 and EUR 1,227.5 per m2 in the no climate and CDS climate impact scenario respectively. These savings are equivalent to average annual savings of EUR 0.67 and EUR 15.34 per m2 in the no climate and climate impact scenario respectively.

### 2.5.2 Impacts on rooftop solar PV generation

Similar to the energy sector, the load factor of rooftop solar PV generation potential is affected by the surrounding air temperature. As temperatures increase beyond the threshold of optimal functioning for rooftop solar PV systems, their efficiency decreases and so does the potential generation.

The equation used for estimating temperature impacts on rooftop solar PV load factor is described below.

*Temperature effect on rooftop solar PV load factor = 1 - IF THEN ELSE ( Mean annual temperature > Temperature threshold for optimal functioning, (Mean annual temperature - Temperature threshold for optimal functioning) * 0.01, 0)*

Figure 47 presents the forecasted generation of 1,000 kW of rooftop solar capacity in kWh in the no climate (red line) and CDS climate impact scenario (blue line). The reductions in generation occur during warmer periods of the year as a consequence of air temperature exceeding the threshold for optimal functioning of solar PV systems.

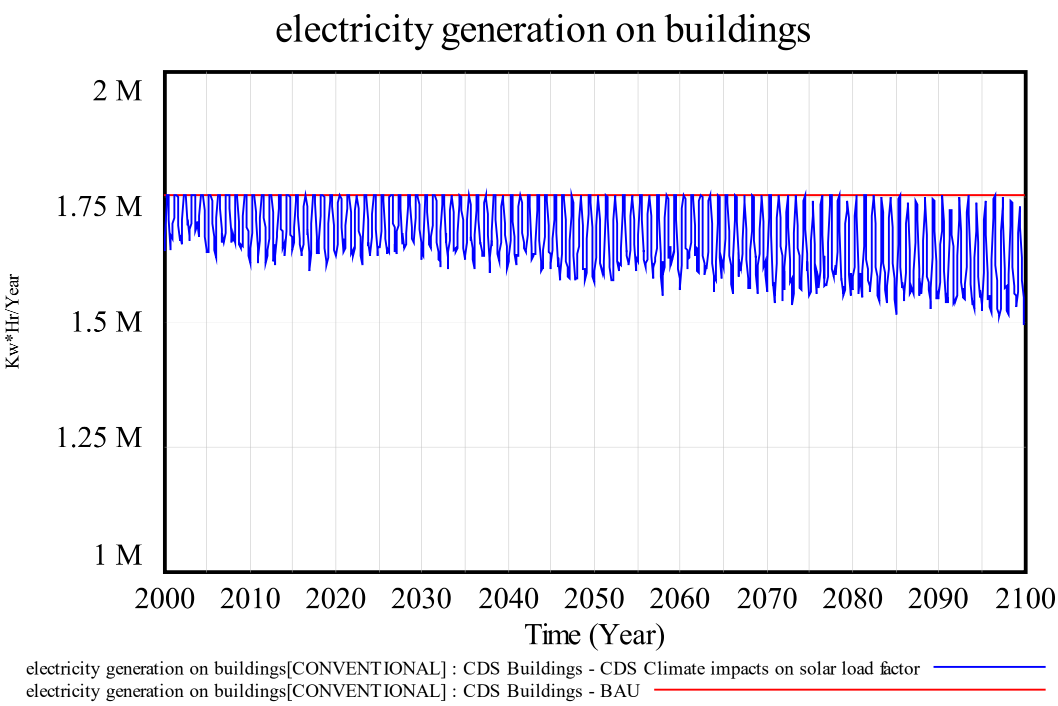


Figure 4: Solar PV generation on buildings for 1 MW of installed capacity

Between 2020 and 2080, the forecasted cumulative generation is 1,683.7 GWh in the no climate scenario and 1,593.5 GWh in the CDS climate impact scenario. The cumulative reduction in generation induced by climate impacts is 90.21 GWh over 80 years, or 1.128 GWh per year on average. This difference in cumulative generation indicates that the average reduction in the load factor of solar PV is 5.4% compared to the no impact scenario.

Assuming a price of 20 cents per kWh, the cumulative savings in electricity cost from using solar energy over 80 years total EUR 336.73 million and EUR 318.69 million in the no climate and CDS climate impact scenario respectively. This is equivalent to average annual reductions in electricity costs of EUR 4.21 million (no climate scenario) and EUR 3.98 million (CDS climate impact scenario). Considering one kW of capacity, the cumulative savings over 80 years are equivalent to EUR 336,730 and EUR 318,690 respectively.

### 2.5.3 Impact of climate on Heating and Cooling Degree Days

Heating and cooling degree days determine the capacity utilization of heating and cooling systems and hence directly affect heating and cooling related energy use and emissions. The approach used for estimating the number of heating and cooling degree days is based on Eurostat (2019). The formulation proposed by Eurostat compares daily temperature values to a minimum threshold to obtain heating degree days (HDD) and a maximum threshold to obtain cooling degree days (CDD). The following formulations are provided (Eurostat, 2019):

*Heating Degree Days =*
*If Tm ≤ 15°C Then [HDD = ∑i(18°C - Tim)] Else [HDD = 0] where Tim is the mean air temperature of day i.*

*Cooling Degree Days = If Tm ≥ 24°C Then [CDD = ∑iTim - 21°C)] Else [CDD = 0]*

Where Tim is the mean air temperature of day i.

Due to the use of monthly data, the number of HDD and CDD is estimated using monthly average daily temperature and the Eurostat thresholds. The equations below describe how climate data is processed to obtain the number of HDD and CDD respectively.

*Heating Degree Days = IF THEN ELSE ( Tair < 15°C, 30, 0)*
*Cooling Degree Days = IF THEN ELSE ( Tair > 24°C, 30, 0)*

The above formulations assume that if the monthly average daily temperature falls under or exceeds the defined thresholds, heating or cooling will be considered for the whole month. Figure 48 presents the forecasts for HDD and CDD in Johannesburg, using the IPSL RCP8.5 scenario. The results indicate that cooling degree days will increase, starting around 2046, while the number of HDD decreases gradually between 2040 and 2085, after which heating seems to occur only in specific months, no longer a season.

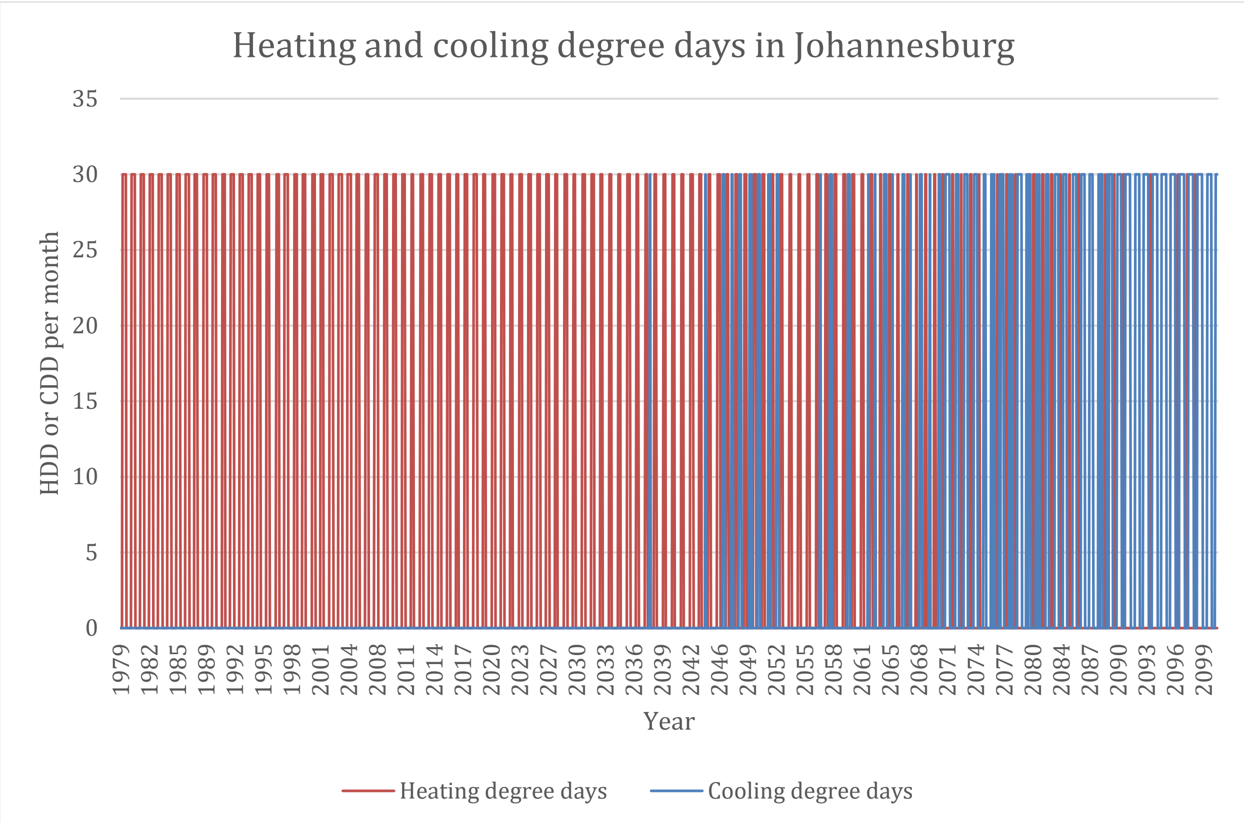


Figure 5: Forecasted Heating Degree Days and Cooling Degree Days in Johannesburg

Table 18 provides information about the forecasted HDD and CDD for Johannesburg in the IPSL RCP8.5 scenario. Compared to 2020-2030, the number of HDD is forecasted to decline by 82% over the next 80 years as a consequence of increasing temperatures. The number of CDD increases from zero (no cooling) to 204 days per year over the next 80 years.

| Indicator | 2020-2030 | 2030-2040 | 2040-2050 | 2050-2060 | 2060-2070 | 2070-2080 | 2080-2090 | 2090-2100 |
|---|---|---|---|---|---|---|---|---|
| Heating degree days | | | | | | | | |
| Climate impact scenario | 111 | 99 | 99 | 90 | 66 | 39 | 36 | 18 |
| *Relative to 2020-2030* | *0%* | *0%* | *0%* | *-9%* | *-33%* | *-61%* | *-64%* | *-82%* |
| No impact scenario | 168 | 168 | 168 | 168 | 168 | 168 | 168 | 168 |
| Cooling degree days | | | | | | | | |
| Climate impact scenario | 0 | 3 | 40 | 33 | 51 | 138 | 144 | 204 |
| *Relative to 2020-2030* | *0%* | *0%* | *1224%* | *988%* | *1588%* | *4489%* | *4689%* | *6691%* |
| No impact scenario | 95 | 95 | 95 | 95 | 95 | 95 | 95 | 95 |

Table 3: Average Heating and Cooling degree days per decade

The changes in HDD and CDD indicated above lead to changes in energy consumption and emissions. Results for key indicators affected by the change in the formulation of heating and cooling degree days are presented in Table 19. Results are presented in cumulative million USD between 2020 and 2100. The results show that the initial setup of the SAVi model was overestimating energy use and related costs and emissions for both heating and cooling. The most significant impact can be seen in the heating sector, where the indicated energy expenditure is 58.5% lower in the CDS climate impact scenario compared to the no impact scenario. For cooling, the reduction in energy cost is 19.2% compared to the no impact scenario.

| Indicator | Heating | | | Cooling | | |
|---|---|---|---|---|---|---|
| | **No impact** | **Climate impact** | **Climate impact vs no impact** | **No impact** | **Climate impact** | **Climate impact vs no impact** |
| Energy expenditure | 183.55 | 76.20 | -58.5% | 6.73 | 5.44 | -19.2% |
| Social cost of carbon | 0.57 | 0.24 | -57.2% | 3.96 | 3.19 | -19.3% |
| **Total costs** | **184.12** | **76.45** | **-58.5%** | **10.68** | **8.63** | **-19.2%** |
| | | | | | | |
| CO2e emissions | 18,421 | 7,888 | -57.2% | 127,659 | 103,036 | -19.3% |
| Energy demand | 614.16 | 21.25 | -96.5% | 182.37 | 147.19 | -19.3% |

Table 4: Key indicators affected by Heating and Cooling Degree Days (in million USD)

# 3 Bibliography


Acclimatise. (2009). *Building Business Resilience to Inevitable Climate Change. Carbon Disclosure Project Report. Global Electric Utilities.* Oxford.

Adeh, E. H., Good, S. P., Calaf, M., & Higgins, C. W. (2019). Solar PV Power Potential is Greatest Over Croplands. *Scientific reports, vol(9), no(1)*, pp. 1-6.

Ahsan, S., Rahman, M. A., Kaneco, S., Katsumata, H., Suzuki, T., & Ohta, K. (2005). Effect of temperature on wastewater treatment with natural and waste materials. *Clean Technologies and Environmental Policy, 7(3)*, 198-202.

Akbari, H. (2005). *Energy saving potentials and air quality benefits of urban heat island mitigation.* Récupéré sur OSTI.org: https://www.osti.gov/biblio/860475/

Akbari, H., Davis, S., Dorsano, S., Huang, J., & Winnett, S. (1992). *Cooling our communities: A guidebook on tree planting and light-colored surfacing.* Washington, DC (United States): Lawrence Berkeley Lab.; Environmental Protection Agency.

Alam, T., Mahmoud, A., Jones, K. D., Bezares-Cruz, J. C., & Guerrero, J. (2019). A Comparison of Three Types of Permeable Pavements for Urban Runoff Mitigation in the Semi-Arid South Texas, USA. *MDPI - Water, 11(10)*.

Allen, R. G., Pereira, L. S., Raes, D., & Smith, M. (2006). *FAO Irrigation and Drainage Paper - Crop Evapotranspiration.* FAO.

Allos, M. (2016, Juin). *Potential Damage Caused by Direct Lightning Strikes*. Récupéré sur Sollatek: https://www.sollatek.com/potential-damage-caused-direct-lightning-strikes/

American Society of Landscape Architects. (2003). *Chicago City Hall Green Roof*. Récupéré sur asla.org: http://www.asla.org/meetings/awards/awds02/chicagocityhall.html

Asian Development Bank. (2012). *Adaptation to Climate Change - The Case of a Combined Cycle Power Plant.* Philippines.

Attia, S. I. (2015). The influence of condenser cooling water temperature on the thermal efficiency of a nuclear power plant. *Annals of Nuclear Energy*, 371-378.

Bartos, M., Chester, M., Johnson, N., Gorman, B., Eisenberg, D., Linkov, I., & Bates, M. (2016). Impacts of rising air temperatures on electric transmission ampacity and peak electricity load in the United States. *Environmental Research Letters, 11(11), 1*.

Basha, M., Shaahid, S. M., & Al-Hadhrami, L. (2011). Impact of fuels on performance and efficiency of gas turbine power plants. *2nd International Conference on Advances in Energy Engineering*, (pp. 558-565). Bangkok.

Bassi, A. M., Pallaske, G., Wuennenberg, L., Graces, L., & Silber, L. (2019, March). *Sustainable Asset Valuation Tool: Natural Infrastructure.* Récupéré sur International Institute for Sustainable Development : https://www.iisd.org/sites/default/files/publications/sustainable-asset-valuation-tool-natural-infrastructure.pdf

Bengtson, H. (2020). *The Rational Method for Estimation of Design Surface Runoff Rate for Storm Water Control*. Récupéré sur brighthubengineering.com: https://www.brighthubengineering.com/hydraulics-civil-engineering/60842-the-rational-method-for-calculation-of-peak-storm-water-runoff-rate/

Bergel-Hayat, R., Debbarh, M., Antoniou, C., & Yannis, G. (2013). Explaining the road accident risk: weather effects. *Accident Analysis & Prevention, 60*, 456-465.

Berghage, R. D., Beattie, D., Jarrett, A. R., Thuring, C., Razaei, F., & O'Connor, T. P. (2009). *Green Roofs For Stormwater Runoff Control.* Cincinnati: EPA.

Bhatt, S., & Rajkumar, N. (2015). Effect of moisture in coal on station heat rate and fuel cost for Indian thermal power plants. *Power Research, 11(4)*, 773-786.
Bhattacharya, C., & Sengupta, B. (2016). Effect of ambient air temperature on the performance of regenerative air preheater of pulverised coal fired boilers. *Int. J. Energy Technology and Policy, Vol. 12, No. 2*, pp. 136–153.
Biswas, B. (2014). Construction and Evaluation of Rainwater Harvesting System for Domestic Use in a Remote and Rural Area of Khulna, Bangladesh. *International Scholarly Research Notices*. doi:https://doi.org/10.1155/2014/751952
Brouwer, C., & Heibloem, M. (1986). Irrigation Water Management and Irrigation Water Needs. *FAO - Training manual, 3.*
Brouwer, C., Prins, K., & Heibloem, M. (1989). *Irrigation water management: irrigation scheduling.* Récupéré sur Fao.org: http://www.fao.org/3/T7202E/t7202e00.htm#Contents
Büyükalaca, O., Bulut, H., & Yılmaz, T. (2001). Analysis of variable-base heating and cooling degree-days for Turkey. *Applied Energy, 69(4)*, pp. 269-283.
Carnegie Mellon University (CMU). (s.d.). *Integrated Environmental Control Model.* Récupéré sur Department of Engineering & Public Policy (EPP): https://www.cmu.edu/epp/iecm/
Chinowsky, P. S., Price, J. C., & Neumann, J. E. (2013). Assessment of climate change adaptation costs for the US road network. *Global Environmental Change, 23(4)*, 764-773.
Chinowsky, P., Hayles, C., Schweikert, A., Strzepek, N., Strzepek, K., & Schlosser, A. (2011). Climate change: comparative impact on developing and developed countries. *The Engineering Project Organization Journal*, pp. 67-80.
Choi, T., Keith, L., Hocking, E., Friedman, K., & Matheu, E. (2011). *Dams and energy sectors interdependency study.*
City of Chicago Department of Environment. (2006). *Green roof test plot project: annual project summary report.* Chicago.
Colman, J. (2013, Avril 26). The effect of ambient air and water temperature on power plant efficiency. *Master Thesis*. Duke University Libraries.
Cronshey, R., McCuen, R. H., Miller, N., Rawls, W., Robbins, S., & Woodward, D. (1986, June). *Urban Hydrology for Small Watersheds.* Récupéré sur USDA-United States Department of Agriculture: https://www.nrcs.usda.gov/Internet/FSE_DOCUMENTS/stelprdb1044171.pdf
Das, T. K., Saharawat, Y. S., Bhattacharyya, R., Sudhishri, S., Bandyopadhyay, K. K., Sharma, A. R., & Jat, M. L. (2018). Conservation agriculture effects on crop and water productivity, profitability and soil organic carbon accumulation under a maize-wheat cropping system in the North-western Indo-Gangetic Plains. *Field Crops Research, 215*, pp. 222-231.
Davies, Z. G., Edmondson, J. L., Heinemeyer, A., Leake, J. R., & Gaston, K. J. (2011). Mapping an urban ecosystem service: quantifying above-ground carbon storage at a city-wide scale. *Journal of applied ecology, 48(5)*, pp. 1125-1134.
Davy, R., Gnatiuk, N., Pettersson, L., & Bobylev, L. (2018). Climate change impacts on wind energy potential in the European domain with a focus on the Black Sea. *Renewable and sustainable energy reviews*, pp. 1652-1659.
De Oliveira, V., De Mello, C., Viola, M., & Srinivasan, R. (2017). Assessment of climate change impacts on the streamflow and hydropower potential in the headwater region of the

Grande river basin, Southeastern Brazil. *International Journal of Climatology 37[15]*, pp. 5005-5023.

De Rosa, M., Bianco, V., Scarpa, F., & Tagliafico, L. A. (2014). Heating and cooling building energy demand evaluation; a simplified model and a modified degree days approach. *Applied Energy, 128*, 217-229.

De Sa, A., & Al Zubaidy, S. (2011). Gas turbine performance at varying ambient temperature. *Applied Thermal Engineering, 31(14-15)*, 2735-2739.

Demuzere, M., Orru, K., Heidrich, O., Olazabal, E., Geneletti, D., Orru, H., . . . Faehnle, M. (2014). Mitigating and adapting to climate change: Multi-functional and multi-scale assessment of green urban infrastructure. *Journal of environmental management, 146*, pp. 107-115.

Dhakal, S., & Hanaki, K. (2002). Improvement of urban thermal environment by managing heat discharge sources and surface modification in Tokyo. *Energy and buildings, 34(1)*, pp. 13-23.

Diaz, C. A., Osmond, P., & King, S. (2015). Precipitation and buildings: estimation of the natural potential of locations to sustain indirect evaporative cooling strategies through hot seasons. *Living and Learning: Research for a Better Built Environment: 49th International Conference of the Architectural Science Association*, (pp. 45-54). Melbourne.

Djaman, K., O'Neill, M., Owen, C. K., Smeal, D., Koudahe, K., West, M., & Irmak, S. (2018). Crop evapotranspiration, irrigation water requirement and water productivity of maize from meteorological data under semiarid climate. *MDPI - Water 2018, 10(4), 405*.

Doorenbos, J., & Kassam, A. (1979). *Yield response to Water Irrigation and Drainage.* Roma: Food and Agricultural Organization; Paper No 33.

Drax. (2017, August 29). *Technology - What hot weather means for electricity*. Récupéré sur Drax.com: https://www.drax.com/technology/hot-weather-means-electricity/

Du, L., Trinh, X., Chen, Q., Wang, C., Wang, H., Xia, X., . . . Wu, Z. (2018). Enhancement of microbial nitrogen removal pathway by vegetation in Integrated Vertical-Flow Constructed Wetlands (IVCWs) for treating reclaimed water. *Bioresource technology, 2*.

Dunn, A. D. (2007). *Green light for green infrastructure.* Récupéré sur Digitalcommons.pace.edu: https://digitalcommons.pace.edu/lawfaculty/494

Durmayaz, A., & Sogut, O. S. (2006). Influence of cooling water temperature on the efficiency of a pressurized-water reactor nuclear-power plant. *International Journal of Energy Research, 30(10)*, pp. 799-810.

East Coast Lightning Equipment INC. (s.d.). *Lightning protection installation cost study* . Récupéré sur East Coast Lightning Equipment INC: https://ecle.biz/coststudy/

Eliasson, J., & Ludvigsson, G. (2000). Load factor of hydropower plants and its importance in planning and design. *11th International Seminar on Hydro Power Plants.* Vienna.

El-Refaie, G. (2010). Temperature impact on operation and performance of Lake. *Ain Shams Engineering Journal 1*, 1-9.

El-Shobokshy, M. S., & Hussein, F. M. (1993). Degradation of photovoltaic cell performance due to dust deposition on to its surface. *Renewable Energy, 3(6-7)*, pp. 585-590.

Engineering ToolBox. (2009). *Pumping Water - Energy Cost Calculator*. Récupéré sur engineeringtoolbox.com: https://www.engineeringtoolbox.com/water-pumping-costs-d_1527.html

Engineering ToolBox. (s.d.). *Hydropower*. Récupéré sur Engineering ToolBox: https://www.engineeringtoolbox.com/hydropower-d_1359.html

EPA. (2014). *The Economic Benefits of Green Infrastructure - A Case Study of Lancaster, PA.*
Eurostat. (2019). *Energy statistics - cooling and heating degree days (nrg_chdd)*. Récupéré sur Eurostat, the Statistical Office of the European Union: https://ec.europa.eu/eurostat/cache/metadata/en/nrg_chdd_esms.htm
Eurostat, the Statistical Office of the European Union. (2019). *Energy statistics - cooling and heating degree days (nrg_chdd)*. Récupéré sur Europa.eu: https://ec.europa.eu/eurostat/cache/metadata/en/nrg_chdd_esms.htm
Evans, D. V., & Antonio, F. D. (1986). Hydrodynamics of Ocean Wave-Energy Utilization: IUTAM Symposium Lisbon/Portugal 1985. *Springer Science & Business Media*, pp. 133-156.
Farkas, Z. (2011). *Considering air density in wind power production.* Budapest.
Fisher, J. C., Bartolino, J. R., Wylie, A. H., Sukow, J., & McVay, M. (2016). *Groundwater-flow model for the Wood River Valley aquifer system, south-central Idaho.* US Geological Survey.
Flowers, M. E., Smith, M. K., Parsekian, A. W., Boyuk, D. S., McGrath, J. K., & Yates, L. (2016). Climate impacts on the cost of solar energy. *Energy Policy, 94*, pp. 264-273.
Gajbhiye, S., Mishra, S. K., & Pandey, A. (2013). Effects of Seasonal/Monthly Variation on Runoff Curve Number for Selected Watersheds of Narmada Basin. *International Journal of Environmental Sciences, Volume 3, No 6*, pp. 2019-2030.
Garfí, M., Pedescoll, A., Bécares, E., Hijosa-Valsero, M., Sidrach-Cardona, R., & García, J. (2012). Effect of climatic conditions, season and wastewater quality on contaminant removal efficiency of two experimental constructed wetlands in different regions of Spain. *Science of the total environment, 437*, pp. 61-67.
Georgi, N. J., & Zafiriadis, K. (2006). The impact of park trees on microclimate in urban areas. *Urban Ecosystems, 9(3)*, pp. 195-209.
Ghamami, M., Fayazi Barjin, A., & Behbahani, S. (2016). Performance Optimization of a Gas Turbine Power Plant Based on Energy and Exergy Analysis. *Mechanics, Materials Science & Engineering Journal, 29*.
GIZ. (2016). *Solar Powered Irrigation Systems (SPIS) – Technology, Economy, Impacts.* Récupéré sur Gesellschaft für Internationale Zusammenarbeit (GIZ): https://energypedia.info/images/temp/2/23/20160630122544!phpeKHVUr.pdf
Gomes, J., Diwan, L., Bernardo, R., & Karlsson, B. (2014). Minimizing the Impact of Shading at Oblique Solar Angles in a Fully Enclosed Asymmetric Concentrating PVT Collector. *Energy Procedia (57)*, pp. 2176-2185.
Good, E., & Calaf, S. (2019). Solar PV Power Potential is Greatest Over Croplands. *SciRep (9, 11442).*
Green, A. (2020). *The intersection of energy and machine learning*. Récupéré sur adgefficiency.com: https://adgefficiency.com/energy-basics-ambient-temperature-impact-on-gas-turbine-performance/
Haerter, J., Hagemann, S., Moseley, C., & Piani, C. (2011). Climate model bias correction and the role of timescales. *Hydrology and Earth System Sciences, 15*, pp. 1065-1073.
Handayani, K., Filatova, T., & Krozer, Y. (2019). The Vulnerability of the Power Sector to Climate Variability and Change: Evidence from Indonesia. *Energies, 12(19), 3640*.
Harrison, G. P., & Whittington, H. W. (2002). Vulnerability of hydropower projects to climate change. *IEE proceedings-generation, transmission and distribution, 149(3)*, pp. 249-255.

Harrison, G., & Wallace, A. (2005). Climate sensitivity of marine energy. *Renewable Energy, 30(12)*, pp. 1801-1817.

Henry, C. L., & Pratson, L. F. (2016). Effects of environmental temperature change on the efficiency of coal-and natural gas-fired power plants. *Environmental science & technology, 50(17)*, 9764-9772.

Hutyra, L. R., Yoon, B., & Alberti, M. (2011). Terrestrial carbon stocks across a gradient of urbanization: a study of the Seattle, WA region. *Global Change Biology, 17(2)*, pp. 783-797.

Ibrahim, S., Ibrahim, M., & Attia, S. (2014). The impact of climate changes on the thermal performance of a proposed pressurized water reactor: nuclear-power plant. *International Journal of Nuclear Energy*.

Jabboury, B. G., & Darwish, M. A. (1990). Performance of gas turbine co-generation power desalting plants under varying operating conditions in Kuwait. *Heat Recovery Systems and CHP, 10(3)*, 243-253.

Jackson, N., & Puccinelli, J. (2006). *Long-Term Pavement Performance (LTPP) data analysis support: National pooled fund study TPF-5 (013)-effects of multiple freeze cycles and deep frost penetration on pavement performance and cost (No. FHWA-HRT-06-121).*

Janssen, H., Carmeliet, J., & Hens, H. (2004). The influence of soil moisture transfer on building heat loss via the ground. *Building and Environment, 39(7)*, 825-836.

Jerez, S., Tobin, I., Vautard, R., Montávez, J. P., López-Romero, J. M., Thais, F., . . . Wild, M. (2015). The impact of climate change on photovoltaic power generation in Europe. *Nature Communications, 6(1)*, pp. 1-8.

Ji, M., Hu, Z., Hou, C., Liu, H., Ngo, H. H., Guo, W., . . . Zhang, J. (2020). New insights for enhancing the performance of constructed wetlands at low temperatures. *Bioresource Technology, 122722*.

JICA. (March 2003). *Manual on flood control planning.* Department of public works and highways.

Jim, C. Y., & Chen, W. Y. (2008). Assessing the ecosystem service of air pollutant removal by urban trees in Guangzhou (China). *Journal of environmental management, 88(4)*, pp. 665-676.

Kadlec, R. H., & Reddy, K. R. (2001). Temperature effects in treatment wetlands. *Water environment research, 73(5)*, pp. 543-557.

Kakaras, E., Doukelis, A., Prelipceanu, A., & Karellas, S. (2006). Inlet air cooling methods for gas turbine based power plants.

Kaldellis, J., & Fragos, P. (2011). Ash deposition impact on the energy performance of photovoltaic generators. *Journal of cleaner production, 19(4)*, pp. 311-317.

Kappos, L., Ntouros, I., & Palivos, I. (1996). Pollution effect on PV system efficiency. *Proceedings of the 5th National Conference on Soft Energy Forms.* Athens.

Kivi, R. (2017, Avril 24). *How Does Geothermal Energy Work?* Récupéré sur Sciencing: https://sciencing.com/geothermal-energy-work-4564716.html

Kloss, C., & Calarusse, C. (2011). *Rooftops to Rivers: Green strategies for controlling stormwater and combined sewer overflows.* New-York.

Koc, C. B., Osmond, P., & Peters, A. (2018). Evaluating the cooling effects of green infrastructure: A systematic review of methods, indicators and data sources. *Solar Energy, 166*, pp. 486-508.

Koch, H., & Vögele, S. (2009). Dynamic modelling of water demand, water availability and adaptation strategies for power plants to global change. *Ecological Economics, 68(7)*, pp. 2031-2039.

Kosa, P. (2011). The effect of temperature on actual evapotranspiration based on Landsat 5 TM Satellite Imagery. *Evapotranspiration, 56(56)*, pp. 209-228.

Krishna, P., Kumar, K., & Bhandari, N. M. (2002). IS: 875 (Part3): Wind loads on buildings and structures-proposed draft & commentary. Document No.: IITK-GSDMA-Wind, 02-V5. Roorkee, Uttarakhand, India: Department of Civil Engineering; Indian Institute of Technology Roorkee.

Kumpulainen, L., Laaksonen, H., Komulainen, R., Martikainen, A., Lehtonen, M., Heine, P., . . . Saaristo, H. (2007 ). *Distribution Network 2030 - Vision of the future power system.* Finland: VTT.

Land, M., Granéli, W., Grimvall, A., Hoffmann, C. C., Mitsch, W. J., Tonderski, K. S., & Verhoeven, J. T. (2016). How effective are created or restored freshwater wetlands for nitrogen and phosphorus removal? A systematic review. *Environmental Evidence, 5*.

Larsen, P., Goldsmith, S., Wilson, M., Strzepek, K., Chinowsky, P., & Saylor, B. (2008). Estimating future costs for Alaska public infrastructure at risk from climate. *Global Environmental Change*, pp. 442-457.

Lavin, P. (2003). *A Practical Guide to Design, Production, and Maintenance for Architects and Engineers.* London/New-York: Spon Press.

Law, Y., Ye, L., Pan, Y., & Yuan, Z. (2012). Nitrous oxide emissions from wastewater treatment processes. *Philosophical Transactions of the Royal Society B: Biological Sciences, 367(1593)*, pp. 1265-1277.

Linnerud, K., Mideksa, T. K., & Eskeland, G. S. (2011). The impact of climate change on nuclear power supply. *The Energy Journal, 32(1)*.

Lise, W., & van der Laan, J. (2015). Investment needs for climate change adaptation measures of electricity power plants in the EU. *Energy for Sustainable Development, 28*, pp. 10-20.

Mamo, G. E., Marence, M., Hurtado, J. C., & Franca, M. J. (2018). Optimization of Run-of-River Hydropower Plant Capacity.

Manoli, G., Fatichi, S., Schläpfer, M., Yu, K., Crowther, T. W., Meili, N., . . . Bou-Zeid, E. (2019). Magnitude of urban heat islands largely explained by climate and population. *Manoli, G., Fatichi, S., Schläpfer, M., Yu, K., Crowther, T. W., Meili, N., ... & Bou-Zeid, E. (2019). Magnitude of urban Nature, 573(7772)*, pp. 55-60.

Manwell, J. F., McGowan, J. G., & Rogers, A. L. (2010). *Wind energy explained: theory, design and application.* John Wiley & Sons.

Manwell, J., McGowan, J., & Rogers, A. (2002). *Wind Energy Explained: Theory, Design and Application.*

Maulbetsch, J. S., & Di Filippo, M. N. (2006). *Cost and value of water use at combined-cycle power plants.* California: California Energy Commission - Public Interest Energy Research Program.

Maupoux, M. (2010). *Solar photovoltaic water pumping.* Récupéré sur Practical Action - The Schumacher Centre for Technology and Development : https://sswm.info/sites/default/files/reference_attachments/MAUPOUX%202010%20Solar%20Water%20Pumping.pdf

Meral, M. E., & Dincer, F. (2011). A review of the factors affecting operation and efficiency of photovoltaic based electricity generation systems. *Renewable and Sustainable Energy Reviews, 15(5)*, pp. 2176-2184.

Mimikou, M. A., & Baltas, E. A. (1997). Climate change impacts on the reliability of hydroelectric energy production. *Hydrological Sciences Journal, 42(5)*, pp. 661-678.

Miradi, M. (2004). Artificial neural network (ANN) models for prediction and analysis of ravelling severity and material composition properties. *CIMCA*, pp. 892-903.

Mirgol, B., Nazari, M., & Eteghadipour, M. (2020). Modelling Climate Change Impact on Irrigation Water Requirement and Yield of Winter Wheat (Triticum aestivum L.), Barley (Hordeum vulgare L.), and Fodder Maize (Zea mays L.) in the Semi-Arid Qazvin Plateau, Iran. *Agriculture, 10(3), 60*.

Mourshed, M. (2012). Relationship between annual mean temperature and degree-days. *Energy and buildings, 54*, pp. 418-425.

N.D. Lea International. (1995). *Modelling Road Deterioration and Maintenance.* Prepared for the Asian Development Bank.

N.D. Lea International. (1995). *Modelling Road Deterioration and Maintenance.* Prepared for the Asian Development Bank.

National Snow & Ice Data Center. (n.d.). *freezing degree-days*. Retrieved from https://nsidc.org/cryosphere/glossary/term/freezing-degree-days

Nazahiyah, R., Yusop, Z., & Abustan, I. (2007). Stormwater quality and pollution loading from an urban residential catchment in Johor, Malaysia. *Water science and technology, 56(7)*, pp. 1-9.

Nemry, F., & Demirel, H. (2012). *Impacts of Climate Change on Transport: A focus on road and rail transport infrastructures.* Luxembourg: Publications Office of the European Union.

Nichol, J. E. (1996). High-resolution surface temperature patterns related to urban morphology in a tropical city: A satellite-based study. *Journal of applied meteorology, 35(1)*, pp. 135-146.

Nordhaus, W. (2017). Revisiting the social cost of carbon. *PNAS*, vol. 11, no.7, 1518-1523.

Nowak, D. J., Greenfield, E. J., Hoehn, R. E., & Lapoint, E. (2013). Carbon storage and sequestration by trees in urban and community areas of the United States. *Environmental pollution, 178, 229-236.*, pp. 229-236.

Ould-Amrouche, S., Rekioua, D., & Hamidat, A. (2010 ). Modelling photovoltaic water pumping systems and evaluation of their CO2 emissions mitigation potential. *Applied Energy, 87*, pp. 3451-3459.

Panagea, I. S., Tsanis, I. K., Koutroulis, A. G., & Grillakis, M. G. (2014). Climate change impact on photovoltaic energy output: the case of Greece. *Advances in Meteorology*.

Pande, P., & Telang, S. (2014). Calculation of Rainwater Harvesting Potential by Using Mean Annual Rainfall, Surface Runoff and Catchment Area. *Green Clean Guide, India, Global Advanced Research Journal of Agricultural Science, Vol 3(7)*, 200-204.

Parker, J. H. (1989, February). The impact of vegetation on air conditioning consumption. *In Proceedings of the Workshop on Saving Energy and Reducing Atmospheric Pollution by Controlling Summer Heat Islands (pp. 45-52).*

Parliamentary Office of Science and Technology (POST). (2011). *Carbon footprint of electricity generation.* Récupéré sur POST Note Update, 383:

https://www.parliament.uk/documents/post/postpn_383-carbon-footprint-electricity-generation.pdf
Pérez, G., Coma, J., Martorell, I., & Cabeza, L. F. (2014). Vertical Greenery Systems (VGS) for energy saving in buildings: A review. *Renewable and Sustainable Energy Reviews, 39*, pp. 139-165.
Petchers, N. (2003). *Combined heating, cooling & power handbook: technologies & applications: an integrated approach to energy resource optimization.* Fairmont Press.
Photovoltaic Softwares. (2020). *Photovoltaic Softwares*. Récupéré sur photovoltaic-software.com: https://photovoltaic-software.com/principle-ressources/how-calculate-solar-energy-power-pv-systems
Pierson Jr, W., & Moskowitz, L. (1964). A proposed spectral form for fully developed wind seas based on the similarity theory of SA Kitaigorodskii. *Journal of geophysical research*, pp. 5181-5190.
Plósz, B. G., Liltved, H., & Ratnaweera, H. (2009). Climate change impacts on activated sludge wastewater treatment: a case study from Norway. *Water Science and Technology, 60(2)*, pp. 533-541.
Poullain, J. (2012). *PDHonline Course H119 (2 PDH) - Estimating Storm Water Runoff.* Récupéré sur pdhonline.org: https://pdhonline.com/courses/h119/stormwater%20runoff.pdf
Prado, R. T., & Ferreira, F. L. (2005). Measurement of albedo and analysis of its influence the surface temperature of building roof materials. *Energy and Buildings, 37(4)*, 295-300.
Rademaekers, K., van der Laan, J., Boeve, S., Lise, W., van Hienen, J., Metz, B., . . . Kirchsteiger, C. (2011). *Investment needs for future adaptation measures in EU nuclear power plants and other electricity generation technologies due to effects of climate change .* Brussels: Library (DM28, 0/36).
Ramos-Scharron, C., & MacDonald, L. (2007). Runoff and suspended sediment yields from an unpaved road segment. *Hydrological Processes, 21(1)*, pp. 35-50.
Rodell, M., Chen, J., Kato, H., Famiglietti, J. S., Nigro, J., & Wilson, C. R. (2007). Estimating groundwater storage changes in the Mississippi River basin (USA) using GRACE. *Hydrogeology Journal 15[1]*, pp. 159-166.
Roorda, J., & van der Graaf, J. (2000). Understanding membrane fouling in ultrafiltration of WWTP-effluent. *Water Science and Technology 41(10-11)*, pp. 345-353.
Rousseau, Y. (2013). Impact of Climate Change on Thermal Power Plants. Case study of thermal power plants in France.
Sahely, H. R., MacLean, H. L., Monteith, H. D., & Bagley, D. M. (2006). Comparison of on-site and upstream greenhouse gas emissions from Canadian municipal wastewater treatment facilities. *Journal of Environmental Engineering and Science, 5(5)*, pp. 405-415.
Saito, I., Ishihara, O., & Katayama, T. (1990). Study of the effect of green areas on the thermal environment in an urban area. *Energy and buildings, 15(3-4)*, pp. 493-498.
Santamouris, M. (2014). Cooling the cities–a review of reflective and green roof mitigation technologies to fight heat island and improve comfort in urban environments. *Solar energy, 103*, pp. 682-703.
Scheehle, E. A., & Doorn, M. R. (2012). *Estimate of United States GHG Emissions from wastewater.* Récupéré sur EPA.org: https://www3.epa.gov/ttn/chief/conference/ei12/green/present/scheele.pdf

Scheehle, E. A., & Doorn, M. R. (2012). *Improvements to the U.S. Wastewater Methane and Nitrous Oxide Emissions.* Récupéré sur EPA.org: https://www3.epa.gov/ttn/chief/conference/ei12/green/scheehle.pdf

Schnetzer, J., & Pluschke, L. (2017). *Solar-Powered Irrigation Systems: A clean-energy, low-emission option for irrigation development and modernization.* FAO.

Shukla, A. K., & Singh, O. (2014). Effect of Compressor Inlet Temperature & Relative Humidity on Gas Turbine Cycle Performance. *International Journal of Scientific & Engineering Research, 5(5)*, 664-670.

Shukla, A. K., & Singh, O. (2014). Effect of Compressor Inlet Temperature & Relative Humidity on Gas Turbine Cycle Performance. *International Journal of Scientific & Engineering Research, 5(5)*, 664-670.

Singh, S., & Kumar, R. (2012). Ambient air temperature effect on power plant performance. *International Journal of Engineering Science and Technology*.

Singh, S., & Tiwari, S. (2019). *Climate Change, Water and Wastewater Treatment: Interrelationship and Consequences.* Singapore: Springer.

Song, Z., Zheng, Z., Li, J., Sun, X., Han, X., Wang, W., & Xu, M. (2006). Seasonal and annual performance of a full-scale constructed wetland system for sewage treatment in China. *Ecological Engineering, 26(3)*, pp. 272-282.

Souch, C. A., & Souch, C. (1993). The effect of trees on summertime below canopy urban climates: a case study Bloomington. *Journal of Arboriculture, 19(5)*, pp. 303-312.

Taha, H. (1996). Modeling impacts of increased urban vegetation on ozone air quality in the South Coast Air Basin. *Atmospheric Environment, 30(20)*, pp. 3423-3430.

Taha, H. (1997). Urban climates and heat islands; albedo, evapotranspiration, and anthropogenic heat. *Energy and buildings, 25(2).*

Taha, H., Akbari, H., & Rosenfeld, A. (1988). Vegetation Canopy Micro-Climate: A Field-Project in Davis, California. *Journal of Climate and Applied Meteorology*.

Taha, H., Akbari, H., & Rosenfeld, A. (1991). Heat island and oasis effects of vegetative canopies: micro-meteorological field-measurements. *Theoretical and Applied Climatology, 44(2)*, pp. 123-138.

Tallis, M., Taylor, G., Sinnett, D., & Freer-Smith, P. (2011). Estimating the removal of atmospheric particulate pollution by the urban tree canopy of London, under current and future environments. *Landscape and Urban Planning, 103(2)*, pp. 129-138.

Tang, H. (2012). Research on Temperature and Salt Migration Law of Sulphate Salty Soil Subgrade in Xinjiang Region. Beijing, China: Beijing Jiaotong University.

Taylor, C. R., Hook, P. B., Stein, O. R., & Zabinski, C. A. (2011). Seasonal effects of 19 plant species on COD removal in subsurface treatment wetland microcosms. *Ecological Engineering, 37(5)*, pp. 703-710.

Tiwary, A., Sinnett, D., Peachey, C., Chalabi, Z., Vardoulakis, S., Fletcher, T., . . . Hutchings, T. R. (2009). An integrated tool to assess the role of new planting in PM10 capture and the human health benefits: A case study in London. *Environmental pollution, 157(10)*, pp. 2645-2653.

Tran, Q. K., Jassby, D., & Schwabe, K. A. (2017). The implications of drought and water conservation on the reuse of municipal wastewater: Recognizing impacts and identifying mitigation possibilities. *Water research, 124*, 472-481.

Tsihrintzis, V. A., & Hamid, R. (1998). Runoff quality prediction from small urban catchments using SWMM. *Hydrological Processes, 12(2)*, pp. 311-329.

U.S. DoE. (2013). *U.S. Energy sector vulnerabilities to climate change and extreme weather.* DOE/PI-0013: U.S. Department of Energy.

U.S. Environmental Protection Agency. (2003, September). *Cooling summertime temperatures: Strategies to reduce heat islands.* Récupéré sur epa.gov: https://www.epa.gov/sites/production/files/2014-06/documents/hiribrochure.pdf

Ullrich, A., & Volk, M. (2009). Application of the Soil and Water Assessment Tool (SWAT) to predict the impact of alternative management practices on water quality and quantity. *Agricultural Water Management, 96(8)*, pp. 1207-1217.

UNEP. (2015). *Economic Valuation of Wastewater - The Cost of Action and the Cost of No Action.* United Nations Environment Programme (UNEP), commissioned by the Global Programme of Action for the Protection of the Marine Environment from Land-based Activities (GPA), through the Global Wastewater Initiative (GW2I).

URS Corporation Limited. (2010). *Adapting Energy, Transport and Water Infrastructure to the Long-term Impacts of Climate Change* . San Francisco, CA, USA, Report RMP/5456.

Valkama, P., Mäkinen, E., Ojala, A., Vahtera, H., Lahti, K., Rantakokko, K., . . . Wahlroos, O. (2017). Seasonal variation in nutrient removal efficiency of a boreal wetland detected by high-frequency on-line monitoring. *Ecological engineering, 98*, pp. 307-317.

Van Vliet, M. T., Yearsley, J. R., Ludwig, F., Vögele, S., Lettenmaier, D. P., & Kabat, P. (2012). Vulnerability of US and European electricity supply to climate change. *Nature Climate Change, 2(9)*, 676-681.

Vought, T. D. (2019, June 30). *An Economic Case for Facility Lightning Protection Systems in 2017*. Récupéré sur VFC: https://vfclp.com/articles/an-economic-case-for-facility-lightning-protection-systems-in-2017/

Watkins, R., Littlefair, P., Kolokotroni, M., & Palmer, J. (2002). The London heat island–Surface and air temperature measurements in a park and street gorges. *ASHRAE Transactions, 108(1)*, pp. 419-427.

Wilbanks, T., Bhatt, V., Bilello, D., Bull, S., Ekmann, J., Horak, W., & Huang, Y. J. (2008). *Effects of Climate Change on Energy Production and Use in the United States.* Lincoln: US Department of Energy Publications.

Xiao, Q., & McPherson, E. G. (2002). Rainfall interception by Santa Monica's municipal urban forest. *Urban ecosystems, 6(4)*, pp. 291-302.

Yamba, F., Walimwipi, H., Jain, S., Zhou, P., Cuamba, B., & Mzezewa, C. (2011). Climate change/variability implications on hydroelectricity generation in the Zambezi River Basin. *Mitigation and Adaptation Strategies for Global Change*, pp. 617-628.

Young, I. R., & Holland, G. J. (1996). Atlas of the oceans: wind and wave climate. *Oceanographic Literature Review, 7(43), 742*.

Yuan, H., Nie, J., Zhu, N., Miao, C., & Lu, N. (2013). Effect of temperature on the wastewater treatment of a novel anti-clogging soil infiltration system. *Ecological engineering, 57*, pp. 375-379.

Zhang, C., Liao, H., & Mi, Z. (2019). Climate impacts: temperature and electricity consumption. *Natural Hazards, 99(3)*, pp. 1259-1275.

Zhang, Y., Kendy, E., Qiang, Y., Changming, L., Yanjun, S., & Hongyong, S. (2004). Effect of soil water deficit on evapotranspiration, crop yield, and water use efficiency in the North China Plain. *Agricultural Water Management, 64*(2), pp. 107-122.

Zhao, C., Liu, B., Piao, S., Wang, X., Lobell, D., Huang, Y., . . . ... (2017). Temperature increase reduces global yields of major crops in four independent estimates. *Proceedings of the National Academy of Sciences, 114 (35)*. doi:https://doi.org/10.1073/pnas.1701762114

Zhao, M., Kong, Z. H., Escobedo, F. J., & Gao, J. (2010). Impacts of urban forests on offsetting carbon emissions from industrial energy use in Hangzhou, China. *Journal of Environmental Management, 91(4)*, pp. 807-813.

Zhao, X., Shen, A., & Ma, B. (2018). Temperature Adaptability of Asphalt Pavement to High Temperatures and Significant Temperature Differences. *Advances in Materials Science and Engineering*.

Zheng, S., Huang, G., Zhou, X., & Zhu, X. (2020). Climate-change impacts on electricity demands at a metropolitan scale: A case study of Guangzhou, China. *Applied Energy, 261, 114295*.

Zhou, Z. C., Shangguan, Z. P., & Zhao, D. (2006). Modeling vegetation coverage and soil erosion in the Loess Plateau Area of China. *Ecological modelling, 198(1-2)*, pp. 263-268.

Zoppou, C. (2001). Review of urban storm water models. *Environmental Modelling & Software, 16(3)*, pp. 195-231.

Zouboulis, A., & Tolkou, A. (2016). Effect of climate change in wastewater treatment plants: reviewing the problems and solutions. Dans S. A. Shrestha, *Managing Water Resources under Climate Uncertainty* (pp. 197-220). Springer.

Zoulia, I., Santamouris, M., & Dimoudi, A. (2009). Monitoring the effect of urban green areas on the heat island in Athens. *Environmental monitoring and assessment, 156(1-4)*.

Zsirai, T., Buzatu, P., Maffettone, R., & Judd, S. (2012, April). *Sludge viscosity—The thick of it*. Récupéré sur The MBR (Membrane Bioreactors): https://www.thembrsite.com/features/sludge-viscosity-in-membrane-bioreactors-the-thick-of-it/

# Annex I: Code for establishing the CDS Toolbox-SAVi link

Code related to offline processing of CDS Toolbox and CDS API data for the C3S_428h_IISD-EU project.

### How does this code relate to the CDS API ?

This code builds on the powerful CDS API but focuses on local impact analysis specific for the C3S_428h_IISD-EU project. It makes it easier to retrieve a time series for a specific location or region, and save the result to a CSV file (a simpler format than netCDF for most climate adaptation practitioners). Additionally, the code combines variables across multiple datasets, aggregate them into asset classes (such as all energy-related variables) and perform actions such as bias correction (use of ERA5 and CMIP5).

### Code available for download

The easy way is to download the zipped archive: - latest (development): https://github.com/perrette/iisd-cdstoolbox/archive/master.zip - or check stable releases with description of changes: https://github.com/perrette/iisd-cdstoolbox/releases (see assets at the bottom of each release to download a zip version)

The hacky way is to use git (only useful during development, for frequent updates, to avoid having to download and extract the archive every time):

- First time: `git clone https://github.com/perrette/iisd-cdstoolbox.git`

- Subsequent updates: `git pull` from inside the repository

### Installation steps

- Download the code (see above) and inside the folder.
- Install Python 3, ideally Anaconda Python which comes with pre-installed packages
- Install the CDS API key: https://cds.climate.copernicus.eu/api-how-to
- Install the CDS API client: pip install cdsapi
- Install other dependencies: conda install --file requirements.txt or pip install -r requirements.txt
- *Optional* dependency for coastlines on plots: conda install -c conda-forge cartopy or see docs
- *Optional* dependency: CDO (might be needed later, experimental): conda install -c conda-forge python-cdo

Troubleshooting: - If install fails, you may need to go through the dependencies in requirements.txt one by one and try either pip install or conda install or other methods specific to that dependency. - In the examples that follow, if you have both python2 and python3 installed, you might need to replace python with python3.

## CDS API

Download indicators associated with one asset class.

**Examples of use**:

```
python download.py --asset energy --location Welkenraedt
```

The corresponding csv time series will be stored in `indicators/welkenraedt/energy`. Note that raw downloaded data from the CDS API (regional tiles in netcdf format, and csv for the required lon/lat, without any correction) are stored under `download/` and can be re-used across multiple indicators.

The `indicators` folder is organized by location, asset class, simulation set and indicator name. The aim is to provide multiple sets for SAVi simulation. For instance, `era5` for past simulations, and various `cmip5` versions for future simulations, that may vary with model and experiment. For instance the above command creates the folder structure (here a subset of all variables is shown):

```
indicators/
  welkenraedt/
    energy/
      era5/
        2m_temperature.csv
        precipitation.csv
        ...
      cmip5-ipsl_cm5a_mr-rcp_8_5/
        2m_temperature.csv
        precipitation.csv
        ...
      ...
```

with two simulation sets `era5` and `cmip5-ipsl_cm5a_mr-rcp_8_5`. It is possible to specify other models and experiment via `--model` and `--experiment` parameters, to add further simulation sets and thus test how the choice of climate models and experiment affect the result of SAVi simulations.

Compared to raw CDS API, some variables are renamed and scaled so that units match and are the same across simulation sets. For instance, temperature was adjusted from Kelvin to degree Celsius, and precipitation was renamed and units-adjusted into mm per month from original (mean_total_precipitation_rate (mm/s) in ERA5, and mean_precipitation_flux (mm/s) in CMIP5). Additionally, CMIP5 data is corrected so that climatological mean matches with ERA5 data (climatology computed over 1979-2019 by default).

Additionally to the files shown in the example folder listing above, figures can also be created for rapid control of the data, either for interactive viewing (`--view-timeseries` and `--view-region`) or or saved as PNG files (`--png-timeseries` and `--png-region`), e.g.

```
python download.py --asset energy --location Welkenraedt --png-timeseries --png-region
```

Single indicators can be downloaded via:

```
python download.py --indicator 2m_temperature --location Welkenraedt
```

The choices available for `--indicator` , `--asset` and `--location` area defined in the following configuration files, respectively:

- controls which indicators are available, how they are renamed and unit-adjusted: indicators.yml (see sub-section below)
- controls the indicator list in each asset class: assets.yml
- controls the list of locations available: locations.yml

Full documentation, including fine-grained controls, is provided in the command-line help:

```
python download.py --help
```

Visit the CDS Datasets download pages, for more information about available variables, models and scenarios:

- ERA5: https://cds.climate.copernicus.eu/cdsapp#!/dataset/reanalysis-era5-single-levels-monthly-means?tab=form

- CMIP5: `https://cds.climate.copernicus.eu/cdsapp#!/dataset/projections-cmip5-monthly-single-levels?tab=form`

In particular, clicking on "Show API request" provides information about spelling of the parameters, e.g. that "2m temperature" is spelled `2m_temperature` and "RCP 8.5" is spelled `rcp_8_5`.

## Indicator definition

This section is intended for users who wish to extend the list of indicators currently defined in indicators.yml. It can be safely ignored for users who are only interested in using the existing indicators.

Let's see how `10m_wind_speed` is defined:

```
- name: 10m_wind_speed
  units: m / s
  description: Wind speed magnitude at 10 m
```

The fields `name` and `units` define the indicator. Description is optional, just to provide some context. It is possible to provide `scale` and `offset` fields to correct the data as `(data + offset) * scale`. Here for `2m temperature`:

```
- name: 2m_temperature
  units: degrees Celsius
  description: 2-m air temperature
  offset: -273.15  # Kelvin to degrees C
```

# denotes a comment to provide some context. Some indicators have different names in ERA5 and CMIP5, and possibly different units. That can be dealt with by providing `era5` and `cmip5` fields, which have precedence over the top-level fields. Here the `evaporation` definition:

```
- name: evaporation
  units: mm per month
  era5:
    name: mean_evaporation_rate  # different name in ERA5
    scale: -2592000  # change sign and convert from mm/s to mm / month
  cmip5:
    scale: 2592000  # mm/s to mm / month
```

In that case both scaling and name depend on the dataset. In CMIP5 which variable name is identical to our indicator name, the `name` field can be omitted. In ERA5, evaporation is negative (downwards fluxes are counted positively), whereas it is counted positively in ERA5.

Indicators composed of several CDS variables can be defined via `compose` and `expression` fields. Let's look at `100m_wind_speed`:

```
- name: 100m_wind_speed
  units: m / s
  description: Wind speed magnitude at 100 m
  era5:
    compose:
      - 100m_u_component_of_wind
      - 100m_v_component_of_wind
    expression: (_100m_u_component_of_wind**2 + _100m_v_component_of_wind**2)
**0.5
  cmip5:
    name: 10m_wind_speed
    scale: 1.6  # average scaling from 10m to 100m, based on one test locatio
n (approximate!)
```

In ERA5, vector components of 100m wind speed are provided. Our indicator is therefore a composition of these two variables, defined by the `expression` field, which is evaluated as a python expression. Note that variables that start with a digit are not licit in python and must be prefixed with an underscore _ in the `expression` field (only there).

For complex expressions, it is possible to provide a `mapping` field to store intermediate variables, for readability. This is used for the `relative_humidity` indicator:

```
- name: relative_humidity
  units: '%'
  era5:
    compose:
```

```
      - 2m_temperature
      - 2m_dewpoint_temperature
    expression: 100*(exp((17.625*TD)/(243.04+TD))/exp((17.625*T)/(243.04+T)))
    mapping: {T: _2m_temperature - 273.15, TD: _2m_dewpoint_temperature - 273
.15}
  cmip5:
    name: near_surface_relative_humidity
```

where T and TD are provided as intermediary variables, to be used in expression.

ERA5-hourly dataset can be retrieved via `frequency: hourly` field, and subsequently aggregated to monthly indicators thanks to pre-defined functions `daily_max`, `daily_min`, `daily_mean`, `monthly_mean`, `yearly_mean`. For instance:

```
- name: maximum_daily_temperature
  units: degrees Celsius
  offset: -273.15
  cmip5:
    name: maximum_2m_temperature_in_the_last_24_hours
  era5:
    name: 2m_temperature
    frequency: hourly
    transform:
      - daily_max
      - monthly_mean
```

This variable is available directly for CMIP5, but not in ERA5. It is calculated from `2m_temperature` from ERA5 hourly dataset, and subsequently aggregated. Note the ERA5-hourly dataset takes significantly longer to retrieve than ERA5 monthly. Consider using in combination with `--year 2000` to retrieve a single year of the ERA5 dataset.

Currently CMIP5 daily is not supported.

### Netcdf to csv conversion

Convert netcdf time series files downloaded from the CDS Toolbox pages into csv files (note: this does not work for netcdf files downloaded via the cds api):

```
python netcdf_to_csv.py data/*nc
```

Help:

```
python netcdf_to_csv.py --help
```

Copernicus Climate Change Service